

# Estimation of the Hip Moment Using a Novel Torque Measurement System and Development and Testing of a One-Sided Robotic Hip Exoskeleton: Preliminary Clinical Investigation

Kishore P\*, Anjan Kumar Dash\*\* and Dilip Kumar K\*\*\*

**Keywords** : Gait Analysis, Inverse Dynamics, Exoskeleton, Torque Sensor.

## ABSTRACT

This research aims to develop a one-sided exoskeleton that can rehabilitate individuals with hemiparesis. The exoskeleton actuator must generate sufficient torque for walking, which requires determining the patient's hip moment. While Inverse dynamics is a standard method for estimating lower limb joint moments, it is challenging for individuals with limited mobility. To address this, a torque measurement system is proposed to find the hip moments during walking. The system is tested on five healthy participants and five participants with hemiparesis. The results of the hip moment obtained from the proposed system are validated using Inverse dynamic analysis. Based on these results, an overground rehabilitation exoskeleton is developed and tested on participants with hemiparesis. The developed exoskeleton improved hip movement and walking parameters, helping participants to walk more naturally. Participants provided positive feedback and expressed confidence while walking with the exoskeleton. These findings show the effectiveness of developed exoskeleton for over-ground rehabilitation.

## INTRODUCTION

Every year, stroke affects around 20 million people worldwide, making it a major cause of long-term disability (Lin et al., 2022). Among these individuals, 15 million will likely experience disabilities, including sensory-motor impairments that affect their gait.

*Paper Received September 2023. Revised October 2024. Accepted November, 2024. Author for Correspondence: Kishore P.*

*\*Research Scholar, School of Mechanical Engineering, SASTRA Deemed to be University, Thanjavur, Tamil Nadu, India.613401.*

*\*\*Professor, School of Mechanical Engineering, SASTRA Deemed to be University, Thanjavur, Tamil Nadu, India.613401.*

*\*\*\* DK Physiotherapy Centre, Thanjavur, Tamil Nadu, India. 613401.*

8,00,000 people have a new or recurrent stroke each year, and many of these individuals require rehabilitation to regain functional independence (Yang et al., 2021). In developing countries like India, stroke is a leading cause of early death and disability (Zhao et al., 2022). Hemiparesis, a manifestation of stroke that affects one side of the body, is common in stroke survivors and can significantly impact their walking ability (Whittle, 2005; Wist et al., 2016).

Repetitive, task-oriented movements and therapist-assisted gait training can enhance muscle strength and coordination in patients with neurological disorders such as hemiparesis. Also, manual assistance from therapists is frequently utilised in stroke rehabilitation to improve walking (Viteckova et al., 2018). However, this method has limitations as manual assistance can hinder the coordination and synchronisation of leg movements and may cause therapist fatigue (Esquenazi et al., 2013). To address the limitation, robotic rehabilitation has evolved and improved symmetrical gait training and reduced the therapist's workload (Sado et al., 2019).

There are three main categories of robotic rehabilitation: Treadmill-assisted rehabilitation, Body weight-supported rehabilitation, and Overground rehabilitation (Shi et al., 2019). Treadmill-assisted rehabilitation robots, such as LOPES, LOKOMAT, ALEX and PIGRO, help people with mobility impairments by providing rehabilitation training through treadmill-based exercises (Belforte et al., 2011; Esquenazi et al., 2017; van Kammen et al., 2020; Veneman et al., 2007; Winfree et al., 2011). These robotic systems are the bilateral exoskeleton, which is attached firmly to the user's leg. Body weight-supported rehabilitation robots assist patients by using a supportive harness that takes up their weight and reduces the load on their legs. This helps them to bear less weight while walking (Riener et al., 2010). This body weight-supported rehabilitation is mainly used by people with spinal cord injuries. Overground rehabilitation robots, such as H2, CORBYS, ReWalk, ReX, and HAL, assist patients in physical therapy and rehabilitation to regain mobility and function following an injury or surgery (Birch et al., 2016;

Bortole et al., 2015; Esquenazi et al., 2012; Kawamoto et al., 2009; Slavnic et al., 2014; Zeilig et al., 2012). These robots are programmed to perform various tasks and exercises to improve strength, balance, and coordination and are typically controlled by a therapist or trained medical professional. The main advantage of overground rehabilitation is that it allows patients to walk on a flat, stable surface that more closely simulates real-world walking conditions (Hwang & Jeon, 2018).

One of the main drawbacks of exoskeleton robots is their cost. These devices are typically quite expensive, which can make them out of reach for many individuals. (Kalita et al., 2021). In addition, exoskeleton robots are quite heavy, which can be a challenge for some users to wear comfortably for extended periods of time (Tan et al., 2021).

This research aims to develop a one-sided overground rehabilitation exoskeleton for persons with hemiparesis with a reduction in weight and cost. The bilateral exoskeleton is heavier in weight as it has a mechanical structure with the actuator at both the lower limb joints. The bilateral exoskeleton is practically not required for people with hemiparesis. (Buesing et al., 2015). People with hemiparesis need support on one side of their body, especially in the hip joint. Also, a one-sided exoskeleton with single actuation at the hip joint further reduces weight and cost (Chen et al., 2020). Moreover, hip exoskeletons offer an additional advantage in terms of user-friendliness, as they are generally easier to use and put on. (Foroutannia et al., 2022). Hence, in this research, the one-sided robotic hip exoskeleton is developed for rehabilitation.

For the successful operation of the exoskeleton and efficient rehabilitation, exoskeleton robots should deliver sufficient torque to actuate the specific joint for the necessary movement. For example, the actuator in the lower limb exoskeleton delivers the moment/torque for hip flexion/extension. If the actuator fails to deliver sufficient torque for the movement, the exoskeleton cannot provide the necessary movement (Yeung & Tong, 2018). Therefore, it is highly necessary to quantify the moment/torque needed to actuate the particular joint segment.

Inverse dynamic analysis is a standard method for calculating joint torque using the kinematics and kinetics of human movement (Hwang & Jeon, 2015, 2018). However, conducting an inverse dynamic analysis on people with hemiparesis can be particularly challenging as it requires gait analysis. The reflective markers typically placed on the lower limb for gait analysis can become dislodged or misplaced during walking. Hence, frequent adjustments and the need to repeat the gait analysis are necessitated, which demands the physical effort required from the patient (Winter, 2009). Hence, to overcome the difficulties in calculating the hip

moments, a torque measurement system has been developed for this research. The proposed system has an integrated LCD unit that provides real-time measurement of hip moments without the need for gait analysis. An inverse dynamic analysis is also conducted in this research to verify the accuracy of the torque measurement system. Based on the peak hip moments obtained from the torque measurement system and inverse dynamic analysis, a one-sided overground rehabilitation exoskeleton is developed to rehabilitate patients with hemiparesis.

## METHODOLOGY

The primary objective for the development of the torque measurement system is to measure the hip moments/torque required for flexion and extension during walking, which is necessary for choosing an actuator for the exoskeleton. Also, an inverse dynamic analysis is performed to validate the results obtained from the developed torque measurement system. Inverse dynamic analysis involves the use of motion capture and force plate data to compute joint moments and forces. The experimentation is conducted with both 5 healthy participants and 5 individuals with hemiparesis. Inclusion criteria for the hemiparetic group are as follows: participants to have experienced a stroke within the past 18 to 24 months. The moderate level of mobility impairment and a walking speed between 0.3 m/s to 0.8 m/s. Cognitive status of Mini-Mental State Examination (MMSE) scores of 24 or higher were included, ensuring that participants could follow instructions and engage in the testing process. Exclusion criteria for hemiparetic participants included severe mobility impairment, significant cognitive impairment (MMSE score below 24), unstable medical conditions, and severe joint deformities. For healthy participants, exclusion criteria included a history of recent lower limb injuries or surgeries and abnormal gait patterns. The Human Studies Department of Thanjavur Medical College, Tamil Nadu, India, approved the conduction of experiments with participants in the laboratory (Approval No. 663). Written consent is obtained from each participant after explaining the nature and purpose of the experiment. Table 1 shows the details of the participants who participated in this research.

Table 1. The details of all study participants

Participant details	Healthy Participants	Participant with hemiparesis
Age (Years)	28±3	40±10
Height (cm)	165±5	165± 8
Gender (Male/Female)	5/0	4/1
Post-stroke (months)	-	18 to 24
Weight (Kg)	68±5	73±10
Type of stroke	-	Ischemic stroke

Also, a one-sided exoskeleton is developed in this research for the rehabilitation training of participants with hemiparesis. The actuator for the

exoskeleton is chosen based on the results obtained from the torque measurement system and the inverse dynamic analysis. The developed exoskeleton is experimented with 3 participants with hemiparesis and 3 healthy participants. The spatiotemporal parameters and the angle of hip flexion and extension during walking with and without an exoskeleton are evaluated to find the efficacy of the exoskeleton in rehabilitation.

## DESIGN AND DEVELOPMENT OF TORQUE MEASUREMENT SYSTEM

As previously mentioned, a torque measurement system has been developed to estimate hip torque/moment needed for flexion and extension. This system has a base, parallel bar, leg frames, hydraulic jack, torque sensor, A.C. servo motor with gearbox, and power and control switches. Figure 1 shows the entire torque measurement system with a person standing on the base and holding the parallel bars. The leg in which the hip moment/torque needs to be measured is attached to the leg frame with flexible straps.

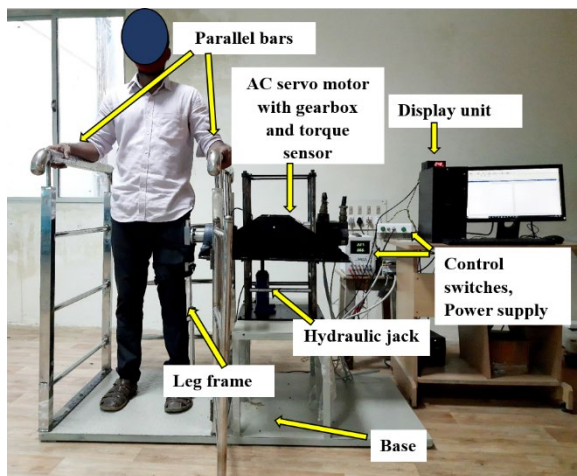
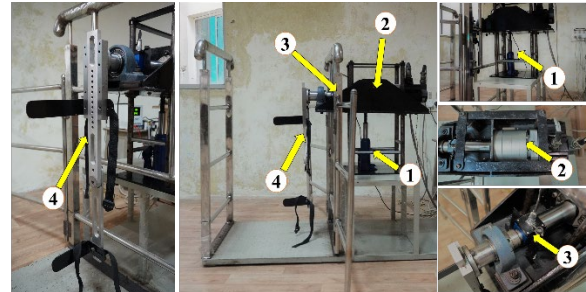


Fig. 1. Fabricated Torque measurement system

Figure 2 shows a detailed view of each component used in the torque measurement system. In Figure 2, label 1 represents the hydraulic jack, which is used to adjust the shaft axis along the hip joint of the participant. Label 2 represents the AC servo motor with a gearbox, and Label 3 represents the torque sensor fitted between the shaft of the AC servo motor and the leg frame. Label 4 represents the leg frame.

The hydraulic jack, positioned under the motor, is used to adjust the height and align the center of the shaft axis with the trochanter point of the hip joint. The AC servo motor is coupled to a planetary gearbox with a 100:1 ratio, producing an output torque of 200 Nm. The leg frame is connected to the output shaft of the AC servo motor through a flange coupling. A rotary torque sensor is placed between the AC servo drive and the flange coupling to the leg frame. This rotary torque sensor is used to measure the hip moment

during flexion and extension. The angle and direction of rotation are fed to the AC servo drives by software, and the reading from the torque sensor can be seen from the LCD display unit and stored in the data acquisition software (Fig. 1).



1- Hydraulic jack, 2- AC servo Motor with gear box  
3- Torque Sensor, 4- Leg frame

Fig. 2 Detailed views of the fabricated torque measurement system

Figure 3 illustrates the dynamic rotary torque sensor (WTQ-1050B-300Nm) that is fitted between the output shaft from the A.C. servo motor with the gearbox and the leg frame. The leg frame is coupled to the flange attached to the output shaft of the A.C. servo motor, as shown in Figure 3. The torque sensor used in this research operated at a sampling frequency of 100 Hz. During flexion and extension, the torque sensor identifies the rotational force and converts the force into an electrical signal for real-time data acquisition. The obtained torque values during testing can be seen in the LCD unit and stored in the data acquisition unit. Hence, the proposed system gives immediate feedback and eliminates the need for complex gait analysis.

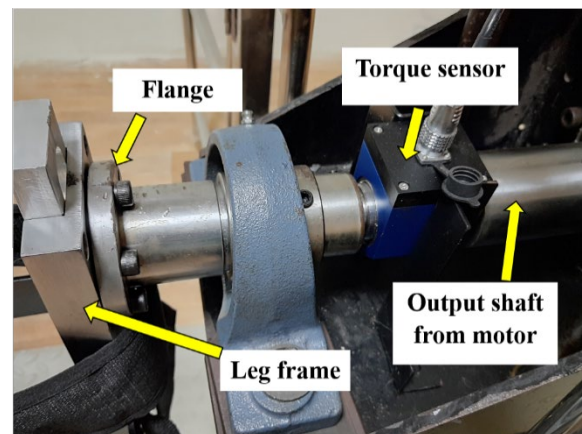


Fig. 3. The torque sensor and leg frame

Figure 4 shows a detailed view of the leg frame. First, the participant whose hip moment needs to be measured stands between the parallel bar, as shown in Figure 1. The hydraulic jack is adjusted to align the shaft axis with the participants' hip joint trochanter point. Then, with the help of flexible straps in the leg frame (Fig. 4), the participants' leg is firmly attached

to the leg frame. The leg frame is designed to be anthropometric, and the height can be adjusted to fit the participant's leg height by using the holes provided in the leg frame, as shown in Figure 4. The knee joint in the leg frame can be locked and unlocked by inserting a pin. Two back supports are attached to the leg frame using threaded bolts at the thigh and shank segments, as shown in Figure 4. These back supports are used to support the leg during flexion and extension. The back supports can be adjusted to fit the participant's leg circumference using the holes provided in the leg frame, as shown in Figure 4. This torque measurement system can test participants with heights ranging from 150 cm to 190 cm.

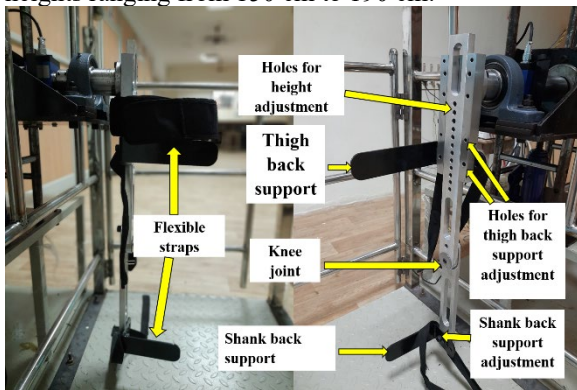


Fig. 4. Detailed view of the leg frame

The 3D model of the leg frame is shown in Figure 5. The leg frame consists of thigh and shank segments with back support at each segment.

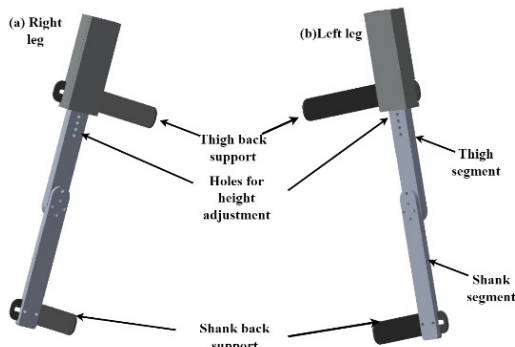


Figure 5. 3D model of leg frame with back support (a) right leg and (b) left leg

The back support can be fixed in two different positions. For example, the back support should be fixed to measure a person's right leg hip moment/torque, as shown in Figure 5a. The motor can then be rotated clockwise for flexion and counterclockwise for extension. Similarly, to measure the left leg hip moment/torque, the back support should be fixed, as shown in Figure 5b, and the motor can be rotated counterclockwise for flexion and clockwise for extension. Therefore, the same leg frame can be used to measure the hip moment/torque for both legs by adjusting the position of the back support.

One advantage of the back support in the leg frame design is that it supports flexion/extension movements. Without back support, the straps in the leg frame would have to pull the leg to the desired angle. This pulling action can cause skin ulcers on the participant, which can be avoided by providing support for moving the leg. The back support in the design provides more convenience and comfort to the participant when lifting the leg.

The Panasonic MMDLT55SF A.C. servo drive and Panatorm V6.0 software control the motor speed, angle, and direction of rotation (clockwise/counterclockwise). Figure 6 illustrates the control architecture of the MMDLT55SF A.C. servo drive. The servo drive is powered by a 24 V, 2A power supply from Scientific India Pvt. Ltd. PSD 3304. The A.C. servo motor has a position encoder for feedback and a braking unit to hold the output at a particular position. The required position and velocity of flexion and extension of the leg are fed into the controller as input using Panatorm V6.0 software. A PID controller is used to control the position, with the difference between the actual position and the desired position being fed back into the controller as an error signal.

Similarly, a PI controller controls the velocity, with the difference between the actual and desired velocity being fed into the controller as input. The current input to the motor is controlled based on the output from both the PI and PID controllers, using a current controller. The controller continues to generate the output until the error value is zero, thereby enabling control of the flexion and extension movement of the hip joint.

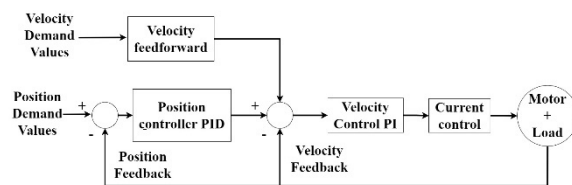


Fig. 6. Control Architecture of the Servo Drive

Figure 7 illustrates the operation of the torque measurement system. Three switches control the system's operation: two push buttons (S1 and S2) and a single-pole dual-throw switch (SPDT). The limit switch acts as a contact breaker for the input power supply to the servo motor. The SPDT switch directs the input power to the S1 or S2 push buttons. The motor rotates clockwise when the power supply is delivered to the S1 push button. The motor rotates counterclockwise when the power supply is given to the S2 push button. The angle of rotation of the motor is programmed using the Panatorm V6.0 software. The required angle of rotation and the acceleration are fed as input to the servo motor from the Panasonic MMDLT55SF A.C. servo drive.

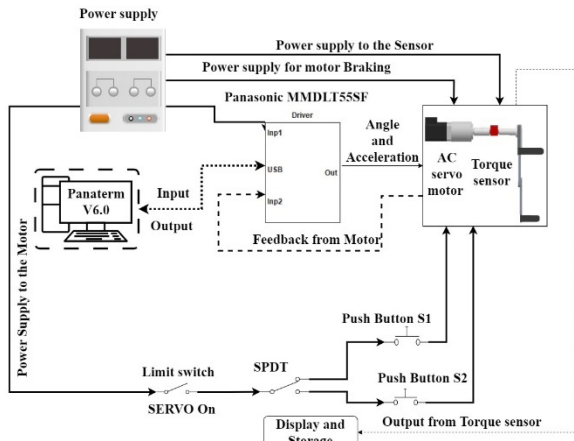


Fig. 7. Operation of torque measurement system Procedure for Measuring the Hip Torque of a Participant.

The cycle starts as follows:

- Power is supplied to the A.C. servo motor (to enable position feedback, braking, and the servo motor), torque sensor, display, and storage unit.
- The participant stands between the parallel bars, and the hydraulic jack below the motor is adjusted to match the shaft's axis to the participant's hip joint. And the leg is firmly attached to the leg frame using the flexible straps
- Panatorm V6.0 software sends the rotation angle for flexion and extension as input to the A.C. servo drive. The limit switch enables the power supply to the SPDT.
- The SPDT switches the power supply to the S1 and S2 push buttons for flexion and extension. The torque sensor continuously detects the users hip torque, and the obtained hip moment can be visually seen in the LCD unit and stored in the data acquisition system.

### INVERSE DYNAMIC ANALYSIS

An inverse dynamic analysis is conducted using an 8 OptiTrack motion capture system and a 3-dimensional force platform. The kinematics of the lower limb segment are obtained from the motion capture system, and the ground reaction force is measured using the force platform.

According to the CODA system, 20 passive reflective markers of 14 mm diameter are placed on the participant's lower limb. Each participant is instructed to walk for 3 complete gait cycles, with one leg/hemiparetic leg landing on the force platform. Kinematics were recorded at 240 Hz, and GRFs at 1000 Hz. Both were synchronised and acquired using Motive software. The synchronised values were then analysed in VISUAL 3D professional software to obtain each segment's linear acceleration, joint angle, and angular accelerations. The following are the assumptions in this analysis.

- The mass of each segment acts downward at the Center of Mass (COM) (Fig.8). Since anteroposterior and mediolateral reaction forces are significantly smaller,

only the vertical Ground Reaction Force (GRF) is taken for the analysis. The vertical GRF passes only through the Center of Pressure (COP) point.

- During walking, the length of each segment and the mass moment of inertia of each segment remain constant. The reaction force at each joint is equal to each segment's mass multiplied by the acceleration due to gravity.

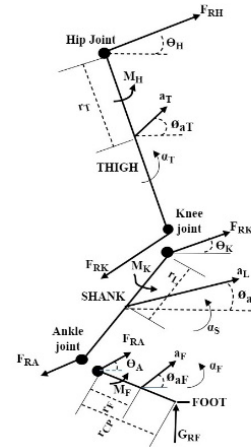


Fig. 8. Freebody diagram of the human lower limb

In Figure 8, the reaction forces and the joint moments at the hip, knee and ankle joints are represented as  $F_{RH}$ ,  $F_{RK}$  and  $F_{RA}$ , and  $M_H$ ,  $M_K$  and  $M_F$ . The angle of the reaction force at each joint is denoted as  $\Theta$ , and the vertical Ground Reaction Force is denoted as  $GRF$ . The distances  $r_T$ ,  $r_L$ , and  $r_F$  represent the distance from the joint to the center of mass of the thigh, shank, and foot segments, and  $r_{cp}$  is the distance from the ankle joint to the CoP. The following equations obtain the moment at the hip joint.

$$M_H = M_k + M_F + m_T g r_T \sin \beta_T + (I_T + m_T r_T^2) \alpha_T \quad (1)$$

The joint moments of the knee and ankle are  $M_K$  and  $M_F$ , respectively, and are determined by the following equations.

$$M_k = M_F + m_s g r_L \sin \beta_k + (I_s + m_s r_L^2) \alpha_s \quad (2)$$

$$M_F = m_F g r_{cp} \cos \beta_F - (G_{RF} r_f) + (I_F + m_F r_f^2) \alpha_F \quad (3)$$

Where  $\beta_T$ ,  $\beta_k$ , and  $\beta_F$  represent the joint angle at the hip, knee and ankle joints.  $I_T$ ,  $I_s$ , and  $I_F$  are a moment of inertia at the thigh, shank and foot segment, and  $\alpha_T$ ,  $\alpha_s$ , and  $\alpha_F$  represent the angular acceleration at the thigh, shank and foot segment. The  $m_t$ ,  $m_s$  and  $m_f$  highlight the mass at the thigh, shank and foot segment (Winter, 2009).

### FINDINGS OF INVERSE DYNAMIC ANALYSIS AND TORQUE MEASUREMENT SYSTEM

Figure 9 depicts the results of the inverse dynamic analysis and the torque measurement system performed on five healthy participants. The hip moments are obtained for one complete gait cycle, starting from heel contact (HC) of the right leg and ending at the subsequent HC.

From the analysis of inverse dynamics and

torque measurement system, it is found that Participants 1 and 2 exerted maximum extension moments of 20.36 Nm and 17.98 Nm, respectively, from both analyses. Similarly, participants 1 and 2 show the maximum flexion moment of 31.2 Nm and 36.55 Nm, respectively. For participants 3, 4, and 5, the maximum moments at flexion are 35.2 Nm, 27.92 Nm, and 29.02 Nm, respectively. The maximum moments at extension are 14.34 Nm, 21.3 Nm, and 21.87 Nm, respectively. From the analysis, it is seen that the maximum moment generated from both analyses nearly matches. Hence, the proposed torque measurement system can be used to find hip moments.

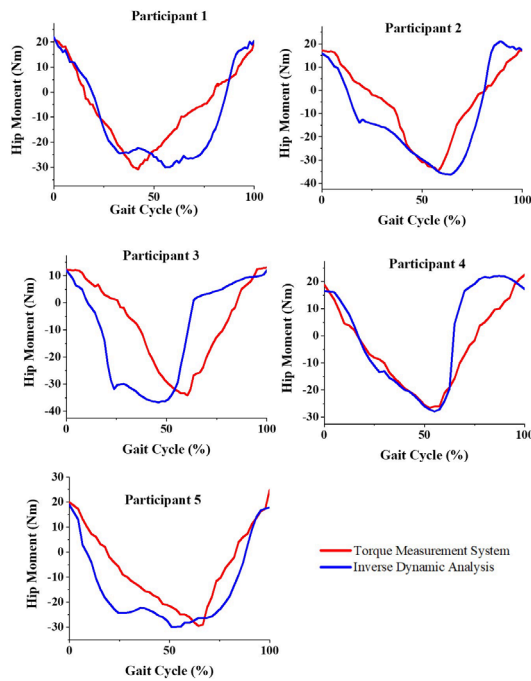


Fig. 9 Hip moments from inverse dynamic and torque measurement system

Figure 10 illustrates the hip moment of participants with hemiparesis for one complete gait cycle obtained from inverse dynamic analysis and torque measurement system. From inverse dynamic analysis, Participants 6 and 7 generated a maximum moment of 22.02 Nm and 18.53 Nm for extending the hip joint, respectively. The maximum moment created for flexing the hip joint is 31.95 Nm and 28.33 Nm, respectively. Similarly, participants 8, 9, and 10 show maximum moments of 12.53 Nm, 4.87 Nm, and 14.97 Nm for extension, and for flexion, the maximum moment generated is 30.45 Nm, 25.5 Nm, and 31.65 Nm.

In the case of peak moments of the torque measurement system (Fig. 10), the maximum moments at flexion are 32.21 Nm, 29.43 Nm, 28.98 Nm, 24.23 Nm, and 31.33 Nm, respectively. Similarly, the maximum moments at extension are 21.9 Nm, 19.23 Nm, 11.89 Nm, 9.5 Nm, and 14.3 Nm, respectively. The moment pattern obtained from both analyses is deviating for persons with hemiparesis. These participants exhibit pathological

gait patterns, such as circumduction and hip hiking, resulting in uneven GRF. This GRF data is the primary influencing factor in inverse dynamic analysis and significantly impacts the calculated hip moment results. Consequently, notable differences in hip moment patterns arise between the two methods. Also, due to limited flexion, they need assistance or support to achieve the flexion/extension angle of the unaffected leg. This support for flexion is provided by the servo actuator in the torque measurement system. Hence, from this analysis, it is clear that the inverse dynamics are not suitable for persons with hemiparesis when calculating the accurate hip moments. The proposed torque measurement system is effective in finding the hip moments.

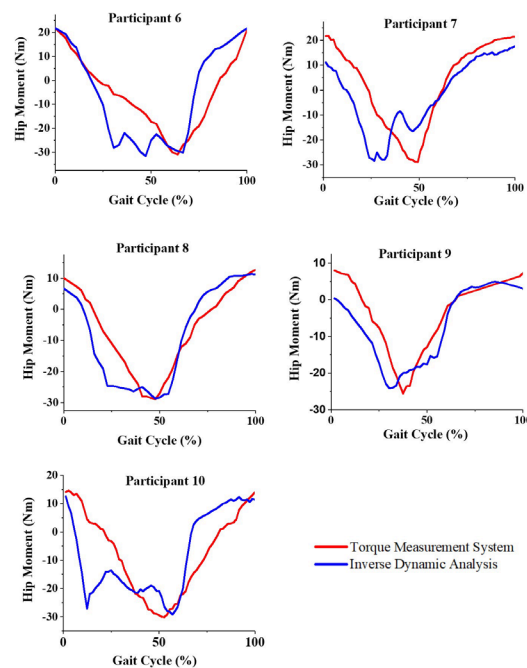


Fig. 10. Hip moments of participants with hemiparesis

Figures 11a and 11b show comparisons of the peak moment during the extension and flexion of a healthy participant, while figures 11c and 15d show the peak moment during the extension and flexion of a participant with hemiparesis.

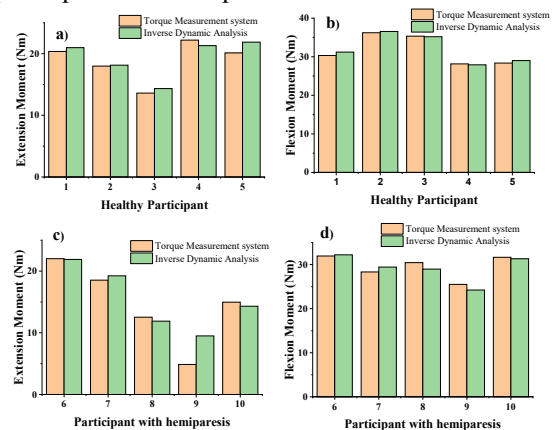


Fig. 11. Comparison of peak hip moments

From the peak hip moment obtained from both analyses, it is evident that a maximum moment of 35 Nm is required for flexion, and 27 Nm is required for extension. Therefore, an actuator with a torque capacity of 40 Nm should be chosen for the exoskeleton to provide the necessary torque for flexion and extension.

### ONE-SIDED EXOSKELETON

With the experimental results of the torque measurement system, a single-sided robotic exoskeleton has been developed for overground rehabilitation. The exoskeleton is designed for the rehabilitation of patients with hemiparesis. It can also be used to compensate for gait in patients with spinal cord injuries. The exoskeleton is actuated only at the hip joint in the sagittal plane and can be used by people with heights ranging from 1.50 to 1.90 cm and a maximum weight of 110 kg. Figure 12 shows the person wearing the developed one-sided robotic exoskeleton. The various parts of the exoskeleton are the controller, actuator, and mechanical structure. The exoskeleton in Figure 12 has a leg shell that fits around the patient's thigh. The leg shell is attached to the exoskeleton's mechanical structure. The exoskeleton's mechanical structure and leg shell are made of polypropylene material to reduce weight. This material is often used in prosthetic and orthotic devices due to its lightweight and higher strength (Aliman et al., 2017; Masood et al., 2016). The flexible straps in the leg shell and harness keep the exoskeleton securely attached to the patient. The exoskeleton's harness is made of aluminium alloy and is padded on both sides for comfort.

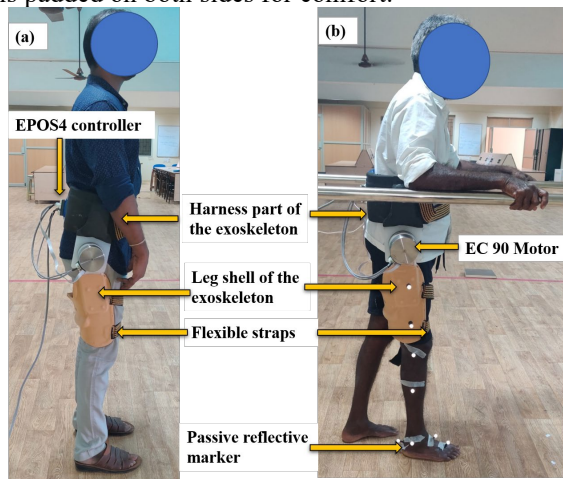


Figure 12. Participants wearing one-sided exoskeleton (a) healthy participant (b) participant with hemiparesis with reflective markers

In this research, the Maxon BLDC EC 90 motor is used for actuating the hip joint. A 24 V DC source powers the motor and has a nominal torque of 444 mNm. Based on the inverse dynamic analysis and torque measurement system results, a maximum

torque of 40 Nm should be chosen to provide the necessary torque for flexion and extension. Therefore, a harmonic drive gearbox with a 100:1 ratio is coupled to the EC 90 motor to provide a net torque of 45 Nm. A power supply with an input of 24 V and 8 A is required for the motor to function. The exoskeleton is powered by a variable DC power supply. The main advantage of using external power instead of a battery is that the exoskeleton can be operated to train the patient for an extended period without needing to replace or recharge the power source. The final weight of the exoskeleton with the electric motor and gearbox is 3 kg.

In this research, the Maxon EPOS4 Position Controller is utilised to control the rotational speed and position of the motor. The control architecture of the exoskeleton is illustrated in Figure 13. Initially, gait analysis is conducted to obtain the kinematics of the lower limb. The gait trajectory of the unaffected side of the participant with hemiparesis is used as input for the controller through a Python program. The motor is equipped with an incremental encoder and hall effect sensor, which provides feedback on its position and velocity. The feedback from the sensors is used to determine the motor's position and velocity, which is then compared with the desired position. The resulting error value is fed into the PID controller, which generates current demand values for the current controller. The current controller regulated the output current to the motor to achieve the required position, velocity, and acceleration. The entire description of the exoskeleton is shown in Table 2.

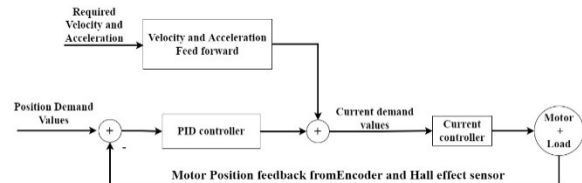


Fig.13 Control architecture of the exoskeleton

Table 2. Specification of the exoskeleton

Parameter	Specification
Device Weight	2.5 kg
Hip Range of Motion	-40° to 40° (max extension flexion angle)
Max. Torque Generation	45 Nm (Actuator capacity for hip joint movement)
Adjustability in Size	Adjustable to fit user height from 150 cm to 190 cm
Control System	Real-time embedded control with PID feedback loops
Sensors	Hall effect Sensors and Encoders
Materials Used	Polypropylene material
Power Source	26 V, 10A AC Power Supply
Max. Operating Speed	20 RPM
Control Algorithm	PID control with adaptive tuning for user-specific gait patterns
Load Capacity	Supports up to 100 kg of user body weight
Sensors frequency	100 Hz

## METHODOLOGY OF TESTING THE EXOSKELETON

This pilot study evaluated the usability of the one-sided robotic hip exoskeleton with 3 healthy participants and 3 participants with hemiparesis. Participants 1 to 3 are healthy participants, and participants 4 to 6 are participants with hemiparesis. Before experimenting with the usability of the exoskeleton with participants, gait analysis is conducted using a motion capture system. The angle of flexion and extension at the hip joint and various spatiotemporal parameters, including speed, stride, step length, step time, stance time, swing time, cycle time, steps per minute, and strides per minute, were evaluated from the gait analysis. The gait analysis result is then used as input to the motor controller to generate a walking trajectory similar to natural walking. For participants with hemiparesis, the walking trajectory of the unaffected side is used as input, as mentioned earlier. Additionally, to verify that participants walking with the exoskeleton followed the same trajectory as the input, a gait analysis is conducted with the participants walking with the exoskeleton. During the experiment, participants were instructed to walk with the exoskeleton and encouraged to take necessary breaks. Three people, including a physiotherapist, were present during the training sessions to ensure the safety of the participants while participants walked with the exoskeleton.

A comprehensive safety protocol is used to ensure the safety and protection of the participants during the exoskeleton testing. First, before testing, the participants are selected based on the inclusion criteria mentioned in section 2. A trained medical professional is present at all times to monitor the participants' health and provide immediate assistance if needed. The supervisor of the testing has an immediate stop action from the control system to halt the device if discomfort or instability occurs. Testing is conducted in a controlled environment with support rails and clear pathways to avoid obstacles. If participants show signs of fatigue, dizziness, pain, or any abnormal physiological responses, such as elevated heart rate, the test is immediately terminated. However, during testing, no such adverse effects were observed. Additionally, the exoskeleton is tested to determine the trajectory without participants checking for malfunction, misalignment, or abnormal behaviour.

## RESULTS OF THE EXOSKELETON

In this research, the exoskeleton is tested with three healthy participants and three participants with hemiparesis. Two different test procedures were conducted to evaluate the performance of the exoskeleton. First, the gait analysis is conducted when the person is walking with the exoskeleton, and second, the gait analysis is performed when the person is walking without the exoskeleton. Donning and doffing the exoskeleton took approximately 3 -5

minutes. Participants are trained on how to use the exoskeleton before the testing. Rest periods were provided between sessions to ensure participants' comfort and safety.

First, the natural gait of the healthy participants is recorded, and the angle of flexion and extension during walking are programmed into the exoskeleton. This is done to check whether the exoskeleton could replicate the same range of flexion and extension as the participant's natural gait. The variation in the angle of hip flexion and extension of the healthy participant on walking with and without the is shown in Figure 14. The green line in Figure 14 represents the flexion and extension angles during walking without the exoskeleton, which serves as the desired trajectory. The orange line represents the angle of flexion and extension while walking with the exoskeleton. From Figure 14, it is evident that all the participants 1, 2, and 3 exhibited a similar angle of flexion and extension when walking with and without the exoskeleton. This confirms that the exoskeleton is programmed to match the natural gait of flexion and extension and achieve the desired trajectory of natural walking. Therefore, it can be concluded that the proposed exoskeleton follows the same walking trajectory as the input.

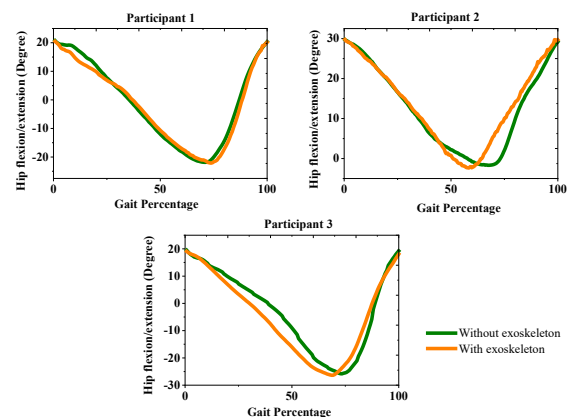


Fig. 14. Variation of hip flexion/extension angle of three healthy participants when walking with and without the exoskeleton

Figure 15 shows that participants 4, 5, and 6 with hemiparesis exhibited an improved angle of flexion and extension when walking with the exoskeleton, compared to their gait with residual deformity. To achieve a symmetrical gait pattern for participants with hemiparesis, the exoskeleton is programmed to follow the walking trajectory of the unaffected leg of the individual, which is considered the desired trajectory (blue line). It is observed from Figure 15 that when the person is walking without the exoskeleton, the flexion and extension angle of the affected leg is minimal (green line). With the help of the exoskeleton, the flexion and extension angles of the affected leg improved, closely following the same trajectory as the healthy leg, with minimal deviation (orange line).

Therefore, it is observed that participants with

hemiparesis exhibit a more symmetrical gait pattern in flexion and extension angles when walking with the exoskeleton. This level of symmetry in gait training is critical for overground rehabilitation, as highlighted in previous studies (Bortole et al., 2015; van Kammen et al., 2020). Continuous rehabilitation with symmetrical angles can enhance the walking ability of individuals over time.

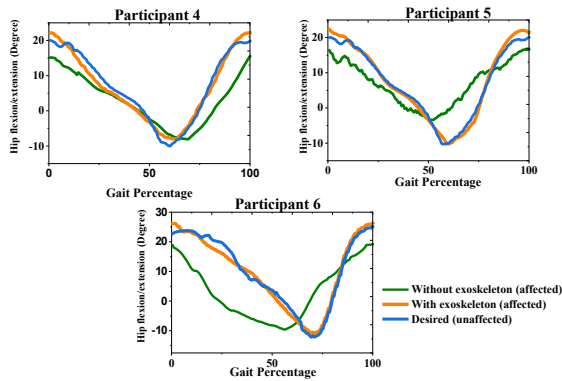


Fig. 15. Variation of hip flexion/extension angle of three participants with hemiparesis when walking with and without the exoskeleton

Table 3 presents the spatiotemporal parameters of healthy participants walking with and without the exoskeleton. Table 4 presents the spatiotemporal parameters of participants with hemiparesis. In Table 3 and Table 4, N represents natural walking without an exoskeleton, and E denotes walking with an exoskeleton. In Table 3, the spatiotemporal parameters of healthy participants are closely matched when walking with and without the exoskeleton. This suggests that participants walking with the proposed robotic exoskeleton can follow a similar trajectory to natural walking for healthy individuals. In the case of participants with hemiparesis (Table 4), gait parameters are improved when walking with the exoskeleton on their affected side compared to natural walking. The exoskeleton improves walking speed, stride length, step length, steps per minute, strides per minute, and temporal parameters for participants with hemiparesis.

Table 3. Spatiotemporal parameter of the healthy participants walking with (E) and without exoskeleton (N)

Parameters	P1		P2		P3	
	N	E	N	E	N	E
Speed (m/s)	0.95	0.96	0.74	0.75	0.92	0.91
Stride (m)	0.19	0.20	0.20	0.21	0.21	0.20
Step Length (m)	0.55	0.53	0.47	0.49	0.50	0.49
Step time (s)	0.58	0.60	0.67	0.62	0.52	0.5
Stance time (s)	0.66	0.69	0.62	0.63	0.65	0.63
Swing time (s)	0.44	0.41	0.53	0.54	0.48	0.50
Cycle time (s)	1.20	1.19	0.96	0.95	1.3	1.4
Steps/Minute	98	98	89.2	90.2	86	87.5
Strides/Minute	68.7	70.5	63.3	62.2	64.6	63.5

Table 4. Spatiotemporal parameter of the participants with hemiparesis walking with (E) and without the exoskeleton (N)

Parameters	P1		P2		P3	
	N	E	N	E	N	E
Speed (m/s)	0.54	0.7	0.50	0.69	0.64	0.65
Stride (m)	0.13	0.1	0.12	0.20	0.15	0.22
Step Length (m)	0.36	0.4	0.3	0.36	0.42	0.45
Step time (s)	0.71	0.5	0.86	0.65	0.66	0.43
Stance time (s)	0.99	0.6	1.24	0.70	0.89	0.77
Swing time (s)	0.59	0.4	0.52	0.45	0.54	0.48
Cycle time (s)	1.37	0.8	1.50	0.85	1.25	0.85
Steps/Minute	85.0	107	70.2	99	92.9	93
Strides/Minute	55.3	77	52	78	64.3	77.9

## DISCUSSION

In this section, the entire discussion on the design and testing of the torque measurement system and the exoskeleton is presented. The main objective of the research is to select an accurate torque rating for the exoskeleton actuator specific to each user. This proper selection of the actuator enables the exoskeleton to follow the required trajectory with sufficient torque. Typically, inverse dynamic analysis is conducted to calculate the lower limb joint moments/torque. This traditional method requires readings from a force plate and motion capture system to obtain the joint kinematics of the lower limb and the ground reaction force (An Introduction to Gait Analysis, 4th Ed. by Michael W. Whittle BSc MSc MB BS PhD (z-Lib.Org), n.d.). A significant drawback of this analysis is that during gait analysis if any marker data is missing due to signal blockage or if the marker is displaced while walking, the experiment needs to be repeated. This can increase the physical effort involved. To overcome this limitation and to accurately determine the hip moments required for flexion and extension, a torque measurement system is proposed in this research. Based on the feedback from the torque measurement system, the exoskeleton actuator is chosen and programmed to match the actual torque required for the flexion and extension movements of the person.

The developed exoskeleton in this research is for overground rehabilitation, and the maximum torque capacity of the exoskeleton actuator is 45Nm. The developed exoskeleton is tested with healthy participants and participants with hemiparesis after sufficient training on the usability of the exoskeleton. For participants with hemiparesis, when walking with the exoskeleton, it is observed that there are improvements in spatiotemporal parameters. Also, there is an enhancement in the flexion and extension angles on the affected side. This improvement in gait parameters highlights that the exoskeleton enhances the walking ability of individuals. The donning and

doffing of the exoskeleton takes approximately 3 to 5 minutes. Another major finding observed in the research is that all participants with hemiparesis exhibited a circumduction gait to provide ground clearance. The exoskeleton facilitates the necessary flexion and extension of the hip joint, allowing participants with hemiparesis to achieve proper ground clearance while walking. This results in a more symmetrical gait pattern when using the exoskeleton (Buurke et al., 2005).

Moreover, participants reported feeling comfortable due to the exoskeleton's design, which is lightweight. Most current exoskeletons weigh between 6 and 12 kg (Wu et al., 2018; Yeung & Tong, 2018) because of their rigid metallic structures, whereas the present exoskeleton weighs approximately 3 kg. This reduced weight is due to the use of polypropylene material, commonly found in orthotic devices. The exoskeleton is securely attached to the participants, and they do not perceive any additional weight. The proposed exoskeleton is suitable for users ranging from 150 to 190 cm in height and weighing up to 100 kg (Bortole et al., 2015). In terms of actuation strength, the device generates a maximum torque of 45 Nm. However, it is programmed to meet the specific torque requirements of each user. Thus, the exoskeleton provides adequate support for hip flexion and extension, which aligns well with the torque requirements identified in prior studies (Hwang & Jeon, 2015, 2018; Liu et al., 2019).

In this pilot study involving 3 participants with hemiparesis and 3 healthy participants tested with the exoskeleton, it is evident that the exoskeleton improved the spatiotemporal parameters and enhanced the angles of flexion and extension of the hip joint for participants with hemiparesis. For healthy participants, the exoskeleton provided a symmetrical gait pattern compared to their natural gait.

The feedback from participants with hemiparesis indicated that they had a positive experience with the robotic exoskeleton. They reported that the device is lightweight and assists in hip flexion and extension, reducing the effort required to flex the hip joint while walking. Participants also noted that the device is comfortable with the adjustable fit, which contributed to their positive experience. All participants with hemiparesis reported that their exoskeleton provided ease of movement and reduced the effort required for hip flexion and extension during walking. In terms of intuitiveness, participants found the device relatively easy to use once they became familiar with it. Some initially required guidance on how to operate the exoskeleton, but after a short learning period, they were able to engage with the device confidently and without difficulty.

Participants also suggested a few areas for enhancement. They mentioned that while the exoskeleton fits securely to the lower limb, adding a bit more padding to the straps of the harness could

increase long-term comfort. Overall, the participants provided positive feedback about the exoskeleton and appreciated its effectiveness and ease of use. They expressed confidence in walking with the exoskeleton and found that it reduced the effort required for walking.

From the research, it can be concluded that the developed exoskeleton helps in the rehabilitation training of patients with hemiparesis. A limitation of this research is that the experimentation is performed with a minimal number of participants. Our future goal is to develop the exoskeleton further, enhancing its ability to respond to user intentions through advanced sensing and adaptive control mechanisms. In future studies, the developed exoskeleton will be tested with a larger and more diverse population to evaluate its efficacy across various degrees of mobility impairment and user needs.

## CONCLUSION

This research presents the development and testing of a one-sided robotic hip exoskeleton for rehabilitating patients with hemiparesis. For the exoskeleton to function effectively, the actuator must provide the required moment at the appropriate time to facilitate necessary movement. The selection of the actuator for the exoskeleton is critical for the flexion and extension of the hip joint. A torque measurement system has been developed as part of this research to address the issue of calculating hip torque for flexion and extension movements. An inverse dynamic analysis is conducted to validate the results of the torque measurement system. The proposed system and inverse dynamic analysis were performed with five healthy participants and five participants with hemiparesis. Both methods revealed that a peak hip moment of 40 Nm is required for flexion and extension movements.

Additionally, a single-sided exoskeleton is developed with a torque capacity of 45 Nm based on the results obtained from the torque measurement system and inverse dynamic analysis. The exoskeleton is mainly used for the overground rehabilitation of hemiparetic patients. At first, the exoskeleton is evaluated with three healthy participants and three individuals with hemiparesis. The results indicate that the proposed exoskeleton improves gait symmetry, enhances flexion and extension angles, and improves spatiotemporal parameters. All participants with hemiparesis showed improvements in the angles of flexion and extension ranging from 10 to 32 degrees when walking with the exoskeleton. The spatiotemporal parameters were also enhanced by 10% to 30%. Moreover, participants with hemiparesis achieved the required ground clearance and exhibited a symmetrical gait pattern while using the exoskeleton. Overall, feedback from the patients who used the exoskeleton was positive, and they reported feeling more confident while walking. In the future, we plan

to assess the exoskeleton's performance in active overground rehabilitation with a larger population.

### ACKNOWLEDGEMENT

We express our gratitude to the Biomedical Device and Technology Development (BDTD), Department of Science and Technology (DST), India, for their financial support in conducting our research. We also extend our thanks to the Research & Modernization (R&M) Fund at SASTRA Deemed to be University for providing the necessary facilities for conducting gait analysis.

### FINANCIAL SUPPORT

This work was supported by the Biomedical Device and Technology Development (BDTD) under the Department of Science and Technology (DST) in India (sanction order number: TDP/BDTD/14/2018).

### REFERENCE

- Aliman, N., Ramli, R., & Haris, S. M. M. (2017). Design and development of lower limb exoskeletons: A survey. In *Robotics and Autonomous Systems* (Vol. 95, pp. 102–116). Elsevier B.V. <https://doi.org/10.1016/j.robot.2017.05.013>
- An Introduction to Gait Analysis, 4th Ed.* by Michael W. Whittle BSc MSc MB BS PhD (z-lib.org). (n.d.).
- Belforte, G., Eula, G., Appendino, S., & Sirolli, S. (2011). Pneumatic interactive gait rehabilitation orthosis: Design and preliminary testing. *Proceedings of the Institution of Mechanical Engineers, Part H: Journal of Engineering in Medicine*, 225(2), 158–169. <https://doi.org/10.1243/09544119JEIM803>
- Birch, N., Graham, J., & Priestley, T. (2016). RAPPER II—Robot-Assisted Physiotherapy Exercises WITH REX-powered walking aid in patients with spinal cord injury. *The Spine Journal*, 16(4), S70. <https://doi.org/10.1016/j.spinee.2016.01.169>
- Bortole, M., Venkatakrishnan, A., Zhu, F., Moreno, J. C., Francisco, G. E., Pons, J. L., & Contreras-Vidal, J. L. (2015). The H2 robotic exoskeleton for gait rehabilitation after stroke: Early findings from a clinical study Wearable robotics in clinical testing. *Journal of NeuroEngineering and Rehabilitation*, 12(1), 1–14. <https://doi.org/10.1186/s12984-015-0048-y>
- Buesing, C., Fisch, G., O'Donnell, M., Shahidi, I., Thomas, L., Mummidisetty, C. K., Williams, K. J., Takahashi, H., Rymer, W. Z., & Jayaraman, A. (2015). Effects of a wearable exoskeleton stride management assist system (SMA®) on spatiotemporal gait characteristics in individuals after stroke: A randomized controlled trial. *Journal of NeuroEngineering and Rehabilitation*, 12(1), 1–14. <https://doi.org/10.1186/s12984-015-0062-0>
- Buurke, J. H., Hermens, H. J., Erren-Wolters, C. V., & Nene, A. V. (2005). The effect of walking aids on muscle activation patterns during walking in stroke patients. *Gait and Posture*, 22(2), 164–170. <https://doi.org/10.1016/j.gaitpost.2004.09.003>
- Chen, B., Zi, B., Qin, L., & Pan, Q. (2020). State-of-the-art research in robotic hip exoskeletons: A general review. *Journal of Orthopaedic Translation*, 20(May 2019), 4–13. <https://doi.org/10.1016/j.jot.2019.09.006>
- Esquenazi, A., Lee, S., Packel, A. T., & Braitman, L. (2013). A Randomized Comparative Study of Manually Assisted Versus Robotic-Assisted Body Weight Supported Treadmill Training in Persons With a Traumatic Brain Injury. *PM and R*, 5(4), 280–290. <https://doi.org/10.1016/j.pmrj.2012.10.009>
- Esquenazi, A., Lee, S., Wikoff, A., Packel, A., Toczylowski, T., & Feeley, J. (2017). A Comparison of Locomotor Therapy Interventions: Partial-Body Weight-Supported Treadmill, Lokomat, and G-EO Training in People With Traumatic Brain Injury. *PM and R*, 9(9), 839–846. <https://doi.org/10.1016/j.pmrj.2016.12.010>
- Esquenazi, A., Talaty, M., Packel, A., & Saulino, M. (2012). The Rewalk powered exoskeleton to restore ambulatory function to individuals with thoracic-level motor-complete spinal cord injury. *American Journal of Physical Medicine and Rehabilitation*, 91(11), 911–921. <https://doi.org/10.1097/PHM.0b013e318269d9a3>
- Foroutannia, A., Akbarzadeh-T, M. R., & Akbarzadeh, A. (2022). A deep learning strategy for EMG-based joint position prediction in hip exoskeleton assistive robots. *Biomedical Signal Processing and Control*, 75. <https://doi.org/10.1016/j.bspc.2022.103557>
- Hwang, B., & Jeon, D. (2015). A method to accurately estimate the muscular torques of human wearing exoskeletons by Torque sensors. *Sensors (Switzerland)*, 15(4), 8337–8357. <https://doi.org/10.3390/s150408337>
- Hwang, B., & Jeon, D. (2018). Estimation of the User's Muscular Torque for an Over-ground Gait Rehabilitation Robot Using Torque and Insole Pressure Sensors. *International Journal of Control, Automation and Systems*, 16(1), 275–283. <https://doi.org/10.1007/s12555-016-0545-1>
- Kalita, B., Narayan, J., & Dwivedy, S. K. (2021). Development of Active Lower Limb Robotic-Based Orthosis and Exoskeleton Devices: A Systematic Review. In *International Journal of Social Robotics* (Vol. 13, Issue 4, pp. 775–793). Springer Science and Business Media B.V. <https://doi.org/10.1007/s12369-020-00662-9>
- Kawamoto, H., Hayashi, T., Sakurai, T., Eguchi, K., & Sankai, Y. (2009). Development of single leg version of HAL for hemiplegia. *Annual International Conference of the IEEE Engineering in Medicine and Biology Society. IEEE Engineering in Medicine and Biology Society. Annual International Conference*, 2009, 5038–5043. <https://doi.org/10.1109/IEMBS.2009.5333698>
- Lin, Q., Ye, T., Ye, P., Borghi, C., Cro, S., Damasceno, A., Khan, N., Nilsson, P. M., Prabhakaran, D., Ramirez, A., Schlaich, M. P., Schutte, A. E., Stergiou,

- G., Weber, M. A., Beaney, T., & Poulter, N. R. (2022). *Hypertension in stroke survivors and associations with national premature stroke mortality: data for 2.5 million participants from multinational screening campaigns* (Vol. 10). [www.thelancet.com/lancetgh](http://www.thelancet.com/lancetgh)
- Liu, X., Zhou, Z., Mai, J., & Wang, Q. (2019). Real-time mode recognition based assistive torque control of bionic knee exoskeleton for sit-to-stand and stand-to-sit transitions. *Robotics and Autonomous Systems*, *119*, 209–220. <https://doi.org/10.1016/j.robot.2019.06.008>
- Masood, J., Ortiz, J., Fernandez, J., Mateos, L. A., & Caldwell, D. G. (2016). Mechanical design and analysis of light weight hip joint Parallel Elastic Actuator for industrial exoskeleton. *Proceedings of the IEEE RAS and EMBS International Conference on Biomedical Robotics and Biomechatronics, 2016-July*, 631–636. <https://doi.org/10.1109/BIOROB.2016.7523696>
- Riener, R., Lünenburger, L., Maier, I. C., Colombo, G., & Dietz, V. (2010). Locomotor training in subjects with sensori-motor deficits: An overview of the robotic gait orthosis Lokomat. *Journal of Healthcare Engineering*, *1*(2), 197–216. <https://doi.org/10.1260/2040-2295.1.2.197>
- Sado, F., Yap, H. J., Ghazilla, R. A. R., & Ahmad, N. (2019). Design and control of a wearable lower-body exoskeleton for squatting and walking assistance in manual handling works. *Mechatronics*, *63*(October), 102272. <https://doi.org/10.1016/j.mechatronics.2019.102272>
- Shi, D., Zhang, W., Zhang, W., & Ding, X. (2019). A Review on Lower Limb Rehabilitation Exoskeleton Robots. *Chinese Journal of Mechanical Engineering*, *32*(1), 74. <https://doi.org/10.1186/s10033-019-0389-8>
- Slavnic, S., Ristic-Durrant, D., Tschakarow, R., Brendel, T., Tuttemann, M., Leu, A., & Graser, A. (2014). Mobile robotic gait rehabilitation system CORBYS - Overview and first results on orthosis actuation. *IEEE International Conference on Intelligent Robots and Systems*, 2087–2094. <https://doi.org/10.1109/IROS.2014.6942842>
- Tan, K., Koyama, S., Sakurai, H., Teranishi, T., Kanada, Y., & Tanabe, S. (2021). Wearable robotic exoskeleton for gait reconstruction in patients with spinal cord injury: A literature review. In *Journal of Orthopaedic Translation* (Vol. 28, pp. 55–64). Elsevier (Singapore) Pte Ltd. <https://doi.org/10.1016/j.jot.2021.01.001>
- van Kammen, K., Boonstra, A. M., van der Woude, L. H. V., Visscher, C., Reinders-Messelink, H. A., & den Otter, R. (2020). Lokomat guided gait in hemiparetic stroke patients: the effects of training parameters on muscle activity and temporal symmetry. *Disability and Rehabilitation*, *42*(21), 2977–2985. <https://doi.org/10.1080/09638288.2019.1579259>
- Veneman, J. F., Kruidhof, R., Hekman, E. E. G., Ekkelenkamp, R., van Asseldonk, E. H. F., & van der Kooij, H. (2007). Design and Evaluation of the LOPES Exoskeleton Robot for Interactive Gait Rehabilitation. *IEEE Transactions on Neural Systems and Rehabilitation Engineering*, *15*(3), 379–386. <https://doi.org/10.1109/TNSRE.2007.903919>
- Viteckova, S., Kutilek, P., de Boisboissel, G., Krupicka, R., Galajdova, A., Kauler, J., Lhotska, L., & Szabo, Z. (2018). Empowering lower limbs exoskeletons: state-of-the-art. *Robotica*, *36*(11), 1743–1756. <https://doi.org/10.1017/S0263574718000693>
- Whittle, M. W. (2005). *Gait Analysis An Introduction*.
- Winfree, K. N., Stegall, P., & Agrawal, S. K. (2011). Design of a minimally constraining, passively supported gait training exoskeleton: ALEX II. *2011 IEEE International Conference on Rehabilitation Robotics*, 1–6. <https://doi.org/10.1109/ICORR.2011.5975499>
- Winter, D. A. (2009). Biomechanics and Motor Control of Human Movement: Fourth Edition. In *Biomechanics and Motor Control of Human Movement: Fourth Edition*. <https://doi.org/10.1002/9780470549148>
- Wist, S., Clivaz, J., & Sattelmayer, M. (2016). Muscle strengthening for hemiparesis after stroke: A meta-analysis. *Annals of Physical and Rehabilitation Medicine*, *59*(2), 114–124. <https://doi.org/10.1016/j.rehab.2016.02.001>
- Wu, C.-H., Mao, H.-F., Hu, J.-S., Wang, T.-Y., Tsai, Y.-J., & Hsu, W.-L. (2018). The effects of gait training using powered lower limb exoskeleton robot on individuals with complete spinal cord injury. *Journal of NeuroEngineering and Rehabilitation*, *15*(1), 14. <https://doi.org/10.1186/s12984-018-0355-1>
- Yang, F., Lees, J., Simpkins, C., & Butler, A. (2021). Interventions for preventing falls in people post-stroke: A meta-analysis of randomized controlled trials. In *Gait and Posture* (Vol. 84, pp. 377–388). Elsevier B.V. <https://doi.org/10.1016/j.gaitpost.2020.12.034>
- Yeung, L.-F., & Tong, R. K.-Y. (2018). Lower Limb Exoskeleton Robot to Facilitate the Gait of Stroke Patients. In *Wearable Technology in Medicine and Health Care* (Issue 1, pp. 91–111). Elsevier. <https://doi.org/10.1016/B978-0-12-811810-8.00005-1>
- Zeilig, G., Weingarden, H., Zweckner, M., Dudkiewicz, I., Bloch, A., & Esquenazi, A. (2012). Safety and tolerance of the ReWalk™ exoskeleton suit for ambulation by people with complete spinal cord injury: A pilot study. *Journal of Spinal Cord Medicine*, *35*(2), 96–101. <https://doi.org/10.1179/2045772312Y.0000000003>
- Zhao, K., Li, G. zong, Nie, L. yan, Ye, X. ming, & Zhu, G. ying. (2022). Edaravone for Acute Ischemic Stroke: A Systematic Review and Meta-analysis. *Clinical Therapeutics*. <https://doi.org/10.1016/j.clinthera.2022.11.005>